ISSN : 0974 - 7443 Volume 8 Issue 3
CHEMICAL TECHNOLOGY
An Indian Journal
Full Paper
CTAIJ 8(3) 2013 [86-94]

Investigation of nanosized carbon materials containing Fe, Co ions by studying its optical and geometrical properties

Mai M.Khalaf*[1,2], H.C.Ibrahimov[1], E.H.Ismailov[1], Y.H.Yusifov[1], M.Alieva[1]
[1]Institute of Petrochemical Processes, Azerbaijan National Academy of Sciences 30, Khojaly Ave., AZ1025 Baku, (AZERBAIJAN)
[2]Chemistry Department, Faculty of Science, Soag University, 82524 Sohag, (EGYPT)
E-mail : mai_kha1@yahoo.com

ABSTRACT

Carbon materials containing iron, cobalt ions have been prepared by a novel process based on the reaction of aluminum and dicholoroethane in liquid paraffin, modified with the chlorides of Fe (III), and Co (II), and the obtained xerogel designated as Fe/CTC-110 and Co/CTC-110. The resulting materials were deposited by micro plasma chemical vapor deposition (MPCVD) method at 800 °C in inert mixed atmosphere (C_2H_2 and He). The obtained materials from this method were characterized by means of different techniques, such as X-ray fluorescence microscopy (XRFM), X-ray diffraction (XRD), UV-vis spectroscopic studies and Dynamic light scattering analyses (DLS) for particle size determination and size distribution of the targeted samples. The cobalt and iron – carbon nanoparticles have been discussed, and the stability of the formed nanoparticles of these samples have been studied at different temperatures at the range from 18 to 70 °C. UV–visible spectroscopy has been carried out for determination of optical band and the nanoparticles size of the samples. Powder X-ray analysis (XRD) revealed the amorphous structure of these systems before deposition and crystallinity after deposition. X-ray fluorescence microscopy (XRFM) studies revealed the homogeneous distribution of elements over the depth. Overall, the results of size of iron, cobalt- carbon nanoparticles have been compared through time-dependent absorption behavior and UV studies. The morphology of the samples has been studied by using scanning electron microscopy (SEM).

KEYWORDS

Fe/CTC;
Co/CTC;
DLS;
Particle size;
UV- vis;
SEM.

INTRODUCTION

The synthesis and characterization of nanoparticles have attracted increasing attention in recent years because particles with sizes in the range of few nanometers behave differently than larger, nonnanoscale particles. According to specialized literature[1], the two main reasons for this change in behavior are an increase in the surface area/mass ratio and the dominance of quantum size effect as particle size decreases. Such increase in the surface area/mass ratio will result in a corresponding increase in chemical reactivity. On the other hand, as the size of particles is reduced (<10 nm), quantum effects can significantly change optical, magnetic, or

electrical properties. It is known also that in heterogeneous catalysis on carbon- based catalysts, the chemical and physical properties play an important role. They can be modified by metal salts and new catalytic activities can be generated. Amongst the heterogeneous catalysts, alumina matrices have been used as interesting supports for diverse active phases[2-5]. Nanosized particles exhibit different, often enhanced, magnetic, electronic, optical, and reactive properties compared to corresponding bulk materials, making them desirable for applications including catalysis, adsorption, ferrofluids, electronic sensing, medical applications, and drug delivery[6-12]. Specific applications for iron nanoparticles include Fischer–Tropsch catalysts, oxygen reduction catalysts in fuel cells, environmental adsorbents for CO or arsenic, and catalysts for CO oxidation or destruction of polychlorinated dibenzodioxins or dibenzofurans (PCDDs/PCDFs)[7,12-17]. Nanoscale iron particles represent a new generation of environmental remediation technologies that could provide cost-effective solutions to some of the most challenging environmental cleanup problems. Nanoscale iron particles have large surface areas and high surface reactivity. Equally important, they provide enormous flexibility for in situ applications. Research has shown that nanoscale iron particles are very effective for the transformation and detoxification of a wide variety of common environmental contaminants, such as chlorinated organic solvents, organochlorine pesticides, and PCBs. Modified iron nanoparticles, such as catalyzed and supported nanoparticles have been synthesized to further enhance the speed and efficiency of remediation[18]. Cobalt nanoparticles used to enhance the permeability of an insulator layer, it is essential to have the metallic material as isolated particles. Otherwise the insulating properties of the dielectric are compromised. Furthermore, utilizing nanoparticles with size between 20 and 100 nm prevents inducing circulating currents into the particles at frequencies of interest in communication applications[19]. This study suggest that after modifying these carbon based materials with different metal chloride (iron and cobalt) leads to modification in physical and chemical properties of the formed samples and the different techniques which had been used confirmed these results.

EXPERIMENTAL

Preparation

Synthesis of the nanosized carbon materials containing Fe ^{III} ions and Co ^{II} ions as samples

The carbon materials containing Fe ^{III} ions and Co ^{II} ions were modified with metal chloride of Fe (III) and Co (II) [20] in laboratory conditions under atmospheric pressure in a solvent in the mode of «in situ», at a certain ratio of initial components in a round bottom flask (reflux system) at 80-90 ˚C for 22-25h. The obtained gel was cooled and aged in the mother liquor at room temperature for 24 h. After that, the solvent was removed under vacuum, and a final drying was carried out at 100-110 ˚C. The obtained dried xerogels (designated as Fe/CTC-110, Co/CTC-110).

Synthesis of the nanosized carbon materials containing Fe^{III} ions and Co^{II} ions by MPCVD method

Carbon nanosized materials containing iron and cobalt catalysts which synthesized as above were deposited in a MPCVD system (MPCVD75-3 CVD nanocarbon generation equipment). Vacuum was supplied by a combination of a turbo-molecular pump and a rotary pump. Working gases (C_2H_2 and He) were fed into the deposition chamber through mass flow controllers. Pressure in the chamber was controlled by adjusting a valve between the deposition chamber and the vacuum pump. The deposition conditions were adapted after typical condition. The substrate temperature ranges from 600 to 800 ˚C, and the working pressure is about -0.095 MPa. The flow rates of C_2H_2 and He are about 20 and 100 ml/min, respectively. The samples were deposited for 1.5 hour and have a thickness of a few hundred of nanometers. The deposition rate is about 2–6 nm/min. The obtained deposited samples (designated as Fe/CTC-800, Co/CTC-800).

Synthesis of the samples for particle size measurements

The particle size measurements were performed at different temperatures of 18, 20, 25, 30, 40, 50, 60 and 70 ˚C, respectively. 20 ˚C was chosen because this is a temperature commonly used for DLS analysis, and the higher temperature was selected to be just below the dried samples of Fe/CTC -110and Co/CTC.

Full Paper

The samples were equilibrated in a water bath (from 18 to 70 °C) for at least 1 h before the measurements. The solvent dicholoroethane (DCE) was also tempered at the measurement temperatures and were filtered immediately before dilution. After that, the diluted test samples were pipetted in the cuvette and allowed a 3-min temperature equilibration, after which the DLS measurement was promptly started. The DLS method correlates the fluctuations of the average intensity of scattered light over time with the size of particles in suspension. The main quantity measured is the translational diffusion coefficient D, which can be used to determine the apparent particle diameter d by using the Stokes-Einstein equation:

$$D = \frac{k_B T}{3\pi\eta(t)d} \quad (1)$$

where k_B is the Boltzmann constant (1.38×10^{-23} m^2 kg s^{-2} K^{-1}), T is temperature (K), η (t) is viscosity (Pa s), and t = time (s).

Characterization techniques

X-ray fluorescence microscopy (XRF)

Elemental analysis of the samples were performed by using X-ray microscope XGT-7000, Horiba with accelerating voltage of X-ray tube 50kV, the diameter of the incident X-ray beam was 100 microns, and the measurement time was 200 sec. the samples were crushed to powder and pressed. The Full Vacuum mode was used which provides elemental analysis for light elements such as aluminum, with the sample chamber maintained at normal atmospheric pressure.

X-ray diffraction (XRD)

XRD patterns were obtained using TD-3500 diffraction at room temperature. Diffraction patterns were obtained with Ni-filtered Cu Kα radiation (λ = 0.15418 nm), monochromatic X-ray beam, and X-ray tube parameters with 35 kV and 25 μA.

UV-Vis-Spectroscopy

Stability of iron and cobalt catalysts supported on Carbon nanostrucured were measured for particle size by UV– VIS spectral analysis, performed on Helios omega UV/VIS spectrophotometer.

Dynamic light scattering particle size (DLS)

The DLS analyses were carried out by the dynamic light scattering particle size analyzer LB-550 Horiba. The particle size measurements were conducted at a fixed 90° angle and a wavelength of 635 nm. The samples were measured at 25 °C which was chosen as this temperature is commonly used for DLS analysis, and 1, 2-dichloroethane was used as a dispersant solvent. To maximize the accuracy of the measurement, the samples were diluted before the DLS analysis by using the solvent mentioned above.

Scanning electron microscopy (SEM)

In order to observe any changes in surface morphologies of the samples, the specimens were analyzed by using scanning electron microscope (JEOL, model 5300).

RESULTS AND DISSCUSSION

DLS analysis

From DLS results (TABLE 1), it is obvious that the temperature had a significant effect on the measured effective diameter of the samples of Fe/CTC -110 and Co/CTC-110. The particle size and poly dispersity of Fe/CTC -110 samples at first from temperature of 18 to 25 °C increased, after that decreased as temperature increased. The effective diameter of Fe/CTC -110 diluted with DCE was about 90% with diameter 46.2 nm at 18 °C, 146.6 nm at 20°C, 143.6 nm at 30°C, and 57.2 at 70°C. This trend was justified by the increased strength of hydrophobic bonds with increasing temperature. and for the sample Co/CTC -110was about 90% with diameter 78.9 nm at 18 °C, 77.5 nm at 20 °C, 79.9 nm at 30 °C, and 95.3 at 70 °C, it was found that the diameter decreased at 20 °C, but it did increase at 70°C, possibly because of precipitation of amorphous Co/CTC -110at that temperature. Figure 1 shows the different particle size distributions Fe /CTC and the Co/CTC -110 depending on the composition at different temperature measurements. The results from DLS indicated that the scattering angle had some effect on the hydrodynamic diameter of the samples of the samples of iron and cobalt. This is due to the fact that the larger particles within a polydispersed sample scatter preferentially in the forward direction, and hence become more represented when the scattering angle is decreased[21]. The effective diameter was virtually constant through-

out the measurement, indicating that the nanoparticles of these systems maintained their structure and size over the duration of the experiment (Figures 2, 3). For the Co/CTC -110samples a slight decreasing trend was observed at 40 ˚C, but it did increase slightly over time after this temperature, and for Fe/CTC -110 samples it was observed that there is a sharp decrease in the diameter of iron nanoparticles at 40 ˚C as mentioned above. Figure 4 shows the nanoscale particles can comprise iron aluminum carbide particles at 800 ˚C having an average particle size of from about 35 to 139 nm in comparison with Fe/CTC at 110 ˚C having an average particle size of from about 50.5 to 194.5 nm. Alternatively, the nanoscale particles can comprise cobalt aluminum carbide particles having an average particle size of from about 30 to 144 nm in comparison with Co/CTC at 110 ˚C having an average particle size of from about 42.7 to 166.7 nm. From these results it was observed that there is a dramatic decrease in the particle size with increase in the temperature due to the lost of solvent and chloride salts and also the particle size is stable at time intervals.

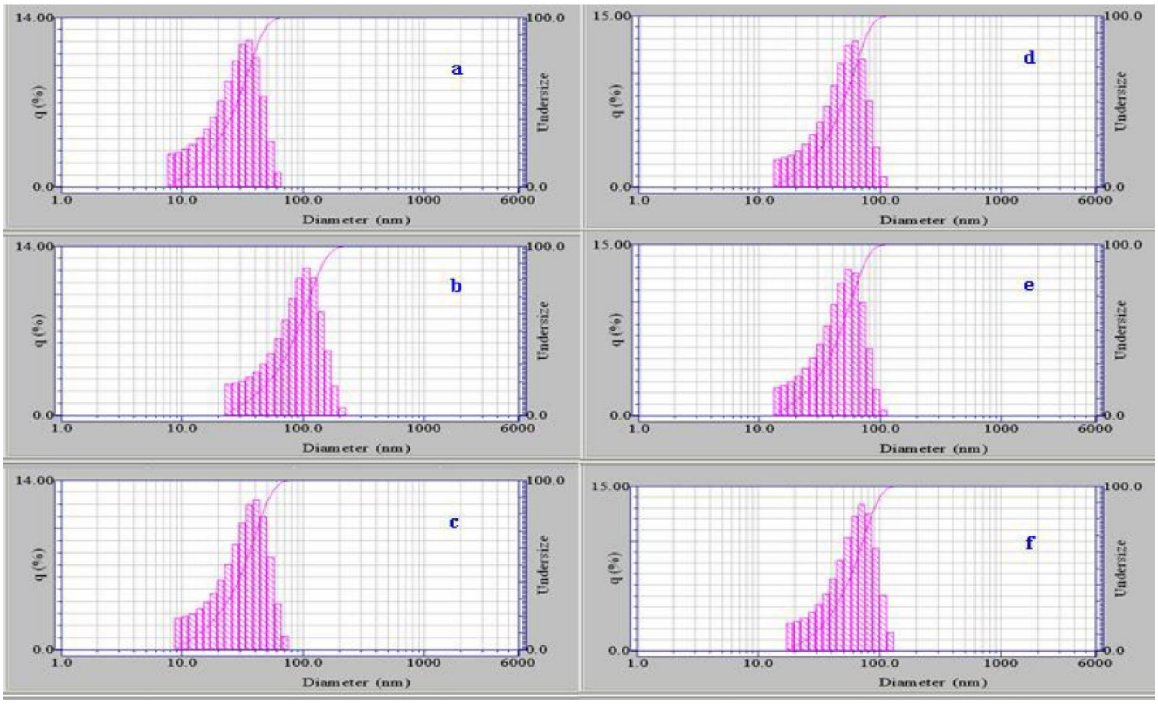

Figure 1 : Particle size distribution of precursor samples at 110 ˚C (a) Fe/CTC-18 (b) Fe/CTC-20 (c) Fe/CTC-70 (d) Co/CTC-18 (e) Co/CTC-20 (f) Co/CTC-70

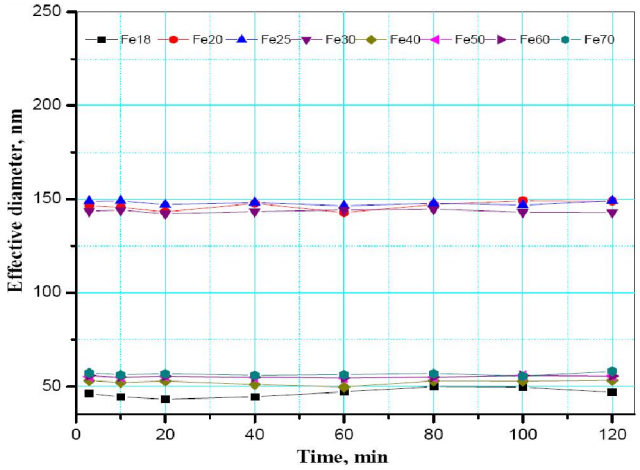

Figure 2 : Dynamics of the effective diameter of Fe/CTC-110 measured

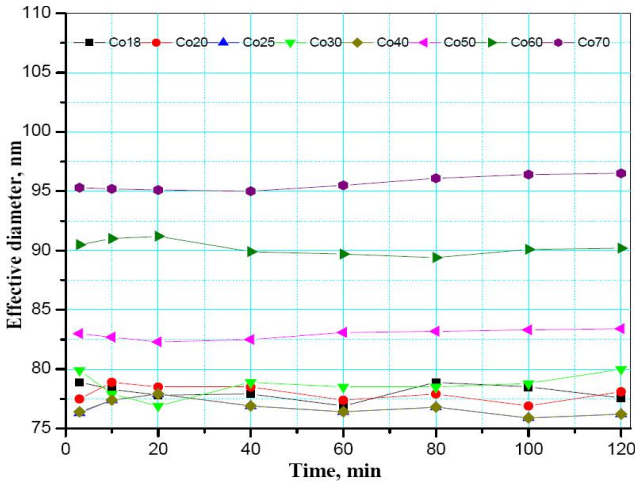

Figure 3 : Dynamics of the effective diameter of Co/CTC-110 measured

Full Paper

TABLE 1 : The particle size distributions, average particle size values, and distribution coefficient of the dried samples at 110 °C under the effect of temperature

Samples name	Diameter on 10%	Diameter on 50%	Diameter on 90%	Diffusion coefficient (m^2/s)
Fe/CTC 18 °C	12.0	28.3	46.2	1.5150×10^{-7}
Fe/CTC 20 °C	36.8	89.4	146.6	4.8236×10^{-8}
Fe/CTC 25 °C	37.5	91.3	148.9	4.7920×10^{-8}
Fe/CTC 30 °C	36.5	87.8	143.6	5.0514×10^{-8}
Fe/CTC 40 °C	13.9	32.8	53.1	1.3879×10^{-7}
Fe/CTC 50 °C	14.2	34.1	55.3	1.3782×10^{-7}
Fe/CTC 60 °C	14.3	34.5	55.8	1.4230×10^{-7}
Fe/CTC 70 °C	15.8	35.8	57.2	1.3921×10^{-7}
Co/CTC 18 °C	21.6	49.7	78.9	8.7405×10^{-8}
Co /CTC 20 °C	21.7	49.2	77.5	8.8254×10^{-8}
Co /CTC 25 °C	21.4	48.5	76.3	9.0870×10^{-8}
Co /CTC 30 °C	22.0	50.6	79.9	8.8116×10^{-8}
Co /CTC 40 °C	21.8	48.8	76.4	9.3376×10^{-8}
Co /CTC 50 °C	23.9	52.6	83.0	8.8983×10^{-8}
Co /CTC 60 °C	25.0	57.4	90.5	8.4538×10^{-8}
Co /CTC 70 °C	27.8	60.8	95.3	8.1748×10^{-8}

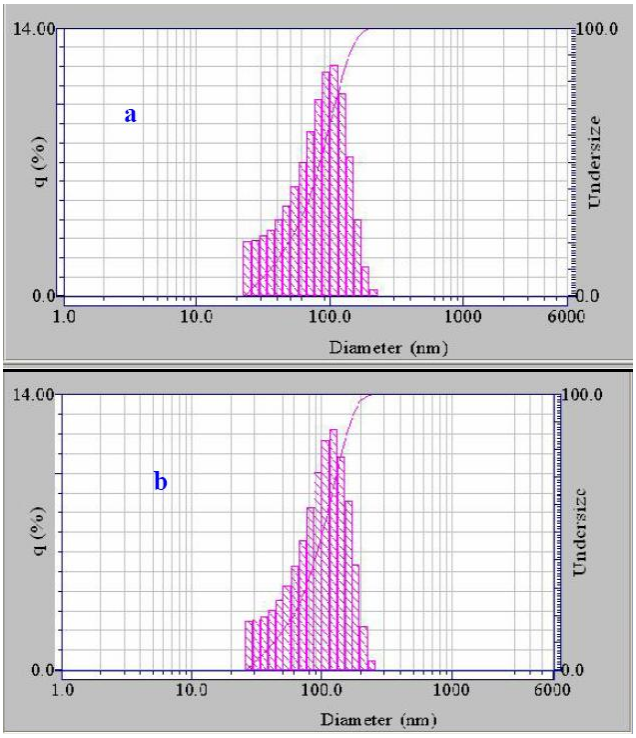

Figure 4 : DLS spectra of samples at 800 °C in He (a) Fe/CTC (b) Co/CTC

UV analysis

UV–vis absorption spectra of Fe/CTC -110and Co/CTC-110 were recorded as shown in Figure 4. Both the curves exhibit well-defined, and give absorption at 364 nm for Fe/CTC -110and at 367 nm for Co/CTC, which is considerably red shifted as compared to Fe/CTC, this shift can be interpreted in terms of a growing process of the Co/CTC -110 nanoparticles and showed also another two bands at 660 and 690 nm. This means that during growth process the particle sizes of some particles of Co/CTC -110 complex increases producing more number of particles that absorb in 600–700 nm region. Stability at different time intervals of Carbon nanosized containing iron and cobalt catalysts Fe/CTC-800 and Co/CTC-800 revealed that these samples, Fe/CTC and Co/CTC remained constant after 2 days, as shown in Figures 5, 6. UV spectrum also confirmed that by deposition of Fe/CTC and Co/CTC at 800 °C in He atmosphere, the characteristic peaks of each sample were shifted to lower wave length at 362 nm for Fe/CTC -800, and at 350 nm for Co/CTC- 800 this can be attributed to the generation of the novel phases of iron and cobalt aluminum carbides as confirmed by XRD results.

XRFM analysis

(XRFM) characterizations revealed that, after heat treatment of these samples at 110 °C, it had been shown (TABLE 2) that the distribution and mass thickness of aluminum, chloride, iron and cobalt elements, respectively, on the surface and over the depth at different positions is rather homogenous throughout the organ-

ism. Figure 8 showed the optical image of Fe/CTC and Co/CTC -110samples at the light and dark points. For samples after thermal treatments at 800 C in inert atmosphere (He) for one hour as shown in TABLE 3, for the complex CTC modified with iron and cobalt chloride the iron aluminide, Fe_3AlC_x and cobalt aluminide, Co_3AlC_x were formed (Figure 9). The data in TABLE 2 showed that, the elemental percentage of carbon for the Fe/CTC and Co/CTC complexes deposited at 800 ˚C in MPCVD is higher than that obtained for samples treated at 110 ˚C as prepared (TABLE 2); this means the formation of Carbon nanostructured containing iron and cobalt nanoparticles at this temperature of higher stability. These results were confirmed by XRD which will be discussed later.

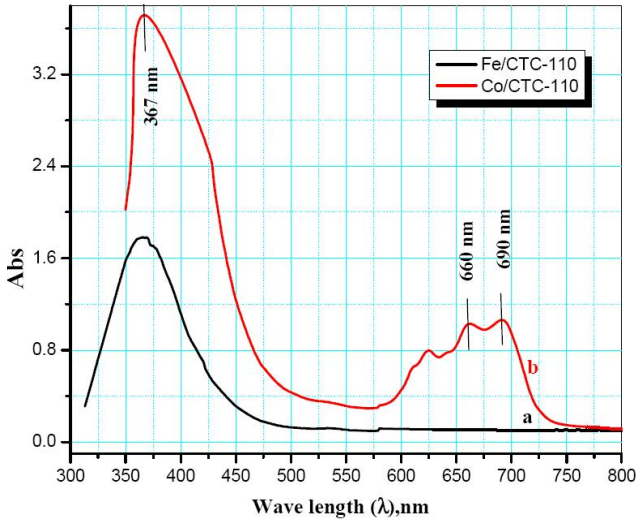

Figure 5 : UV absorbance of as prepared of (a) Fe/CTC and (b) Co/CTC-110 measured at 50 °C

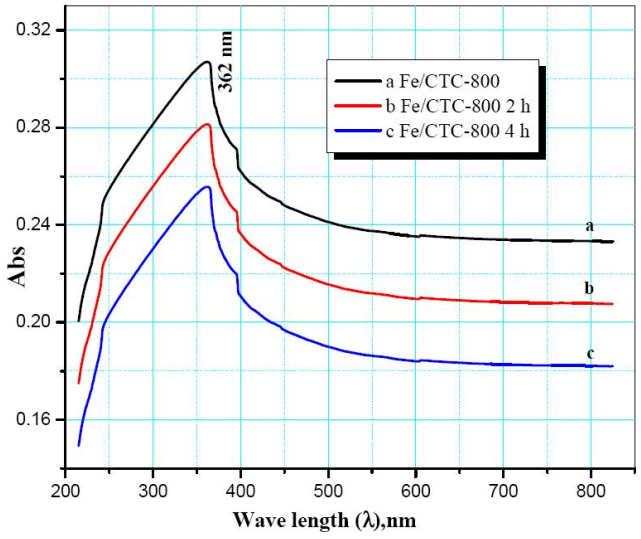

Figure 6 : Stability of Fe/CTC-800 in He at time intervals

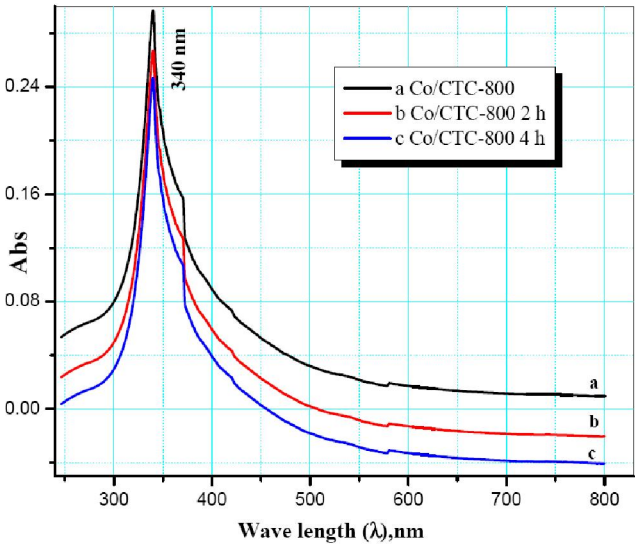

Figure 7 : Stability of Co/CTC-800 in He at time intervals

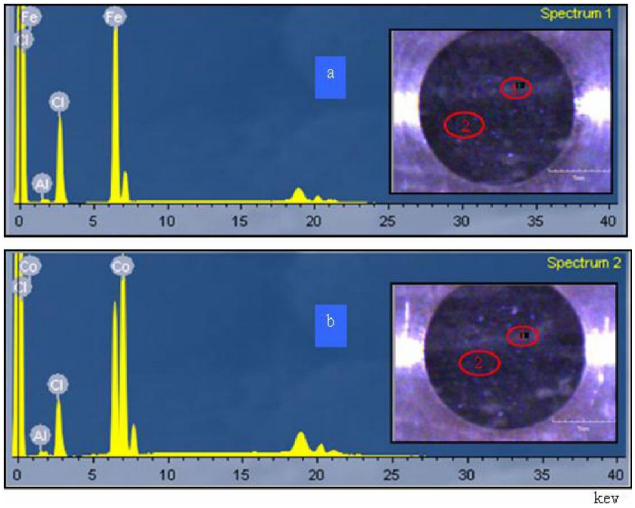

Figure 8 : EDRF analysis and optical image of initial (a) Fe/CTC-110 (b) Co/CTC-110 at (1) light and (2) dark points

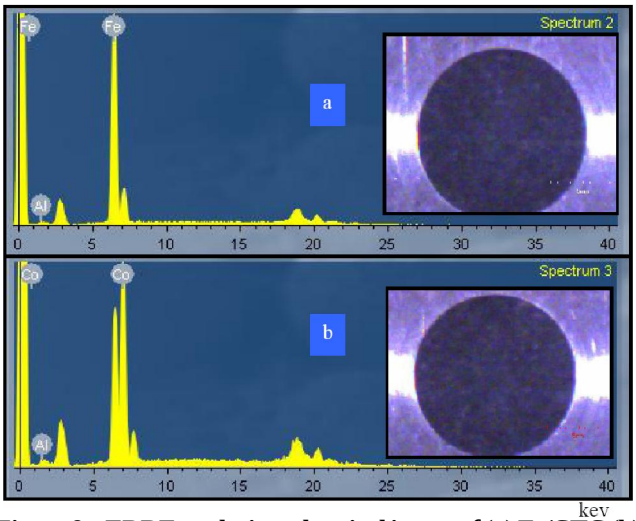

Figure 9 : EDRF analysis and optical image of (a) Fe/CTC (b) Co/CTC complexes treated at 800 °C in He

Full Paper

TABLE 2 : The content of elements (wt. %) in samples treated at 110 °C for 6 hours and their distribution over the depth

Samples name	Elements (wt. %)					The distribution of elements over the depth			
	Al	Cl	*C	Fe	Co	Al	Cl	Fe	Co
light points									
Fe/CTC-110	19.7	31.7	21	27.6	-	0.045	0.178	0.255	-
Co/CTC-110	15	45.4	18.4	-	21.2	0.031	0.214	-	0.305
dark points									
Fe/CTC-110	17.3	33.5	21	28.1		0.048	0.236	0.316	-
Co/CTC-110	14.9	45.6	18.4	-	21.1	0.030	0.217	-	0.303

***C content was determined by the balance of the treatment of the samples at 110 °C.**

TABLE 3 : The content of elements (wt. %) in samples deposited in MPCVD at 800 °C for 1 hour in inert atmosphere (He) and their distribution over the depth

Samples name	Elements (wt. %)				Volatile %	Ash %	The distribution of elements over the depth		
	Al	*C	Fe	Co			Al	Fe	Co
Fe/CTC-800	12.4	30.2	57.4	-	50.7	49.4	0.007	0.218	-
Co/CTC-800	19.9	34.7	-	45.4	54.9	45.1	0.006	-	0.096

*** C content was determined by the balance of the treatment of the samples at 800 °C.**

RD analysis

XRD patterns for the samples Fe/CTC -110and Co/CTC -110 obtained with heat treatment at 110 °C are shown in Figure 10. The patterns showed that we have an amorphous structure for our systems. Figures 11, 12 shows the patterns of nanosized-carbon materials containing Fe, Co ions (Fe/CTC-800 He and Co/CTC-800 He) prepared by the chemical vapor deposition process (MPCVD) in He treated at 800 °C. The patterns for Fe/CTC-800 He show peaks at 2θ = 33.7°, 41.5°, 49.5°, 70.7°, 85.4° of crystalline cubic aluminum iron carbide $AlFe_3C_{0.5}$ phase (file no. 29-0044) corresponds to (110), (111),(102), (220) and (311) planes respectively, as well as at 37.5°, 41.7°, 66.9° and 83.4° of monoclinic iron carbide Fe_2C phase (file no. 17-0897) corresponds to (010), (002), (-126) and (200) planes, further more existence of hexagonal iron Fe as traces (file no. 50-1275) at 49.5 ° corresponds to (102) plane. The patterns for Co/CTC-800 He show peaks at 2θ = 34.3°, 42.3°, 55.6°, 72.3° of crystalline cubic aluminum cobalt carbide $AlCo_3C_{0.5}$ phase (file no. 29-0023) corresponds to (110), (111),(210), and (220) planes respectively.

SEM analysis

The SEM images of the Fe/CTC and Co/CTC samples at 800 °C in inert atmosphere (He gas) showed as illustrated in Figure 13a that the particle size of some grains has ranged from 50 to 100 nm and revealed structural differences, which are probably due to the presence carbon nanoparticles. This synthesized systems comprised large grains, which were embedded in a mixture consisting of small grains as referred in image (Figure 13 a). However, the size of these grains grew larger by agglomeration at this higher temperature. Figure 13b shows the surface plot of a selected area of a SEM image acquired from Fe/CTC at 800 °C in inert He gas. As can be seen the Fe/CTC-800 He sample deposits which appeared heterogeneous in terms of particle size and shape and represented smooth surface over long length scales. However, the more phases for Fe/CTC at 800 °C in inert gas He prevent them from diffusion into bulk and consequently increase its surface plot.

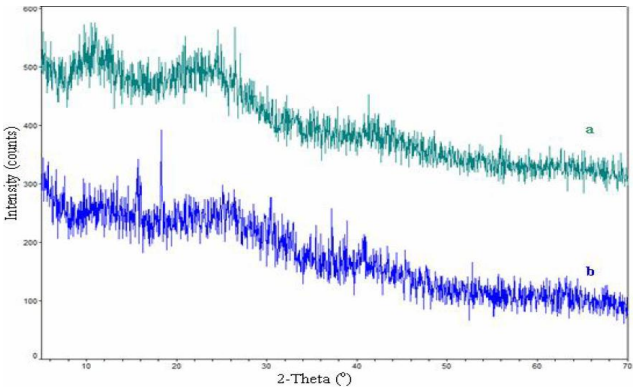

Figure 10 : XRD patterns of precursor samples at 110 °C (a) Fe/CTC (b) Co/CTC

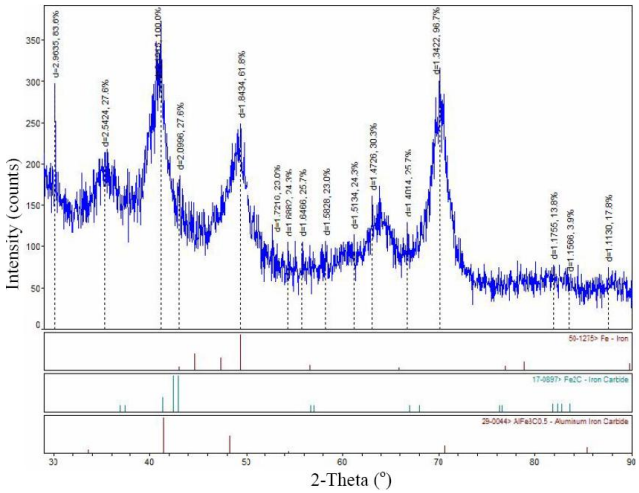

Figure 11 : XRD patterns of Fe/CTC deposited in MPCVD at 800 ˚C in He

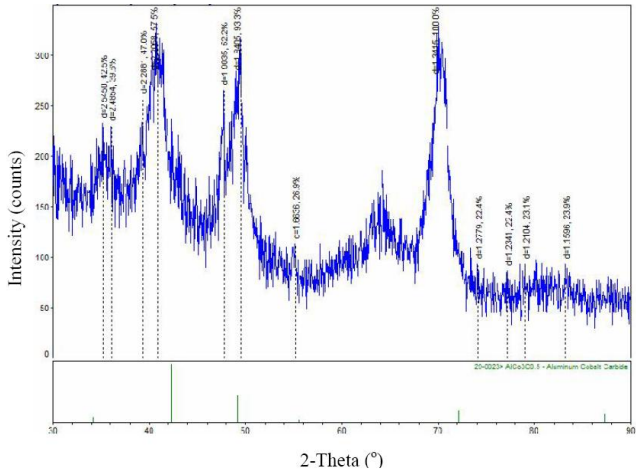

Figure 12 : XRD patterns of Co/CTC deposited in MPCVD at 800 ˚C in He

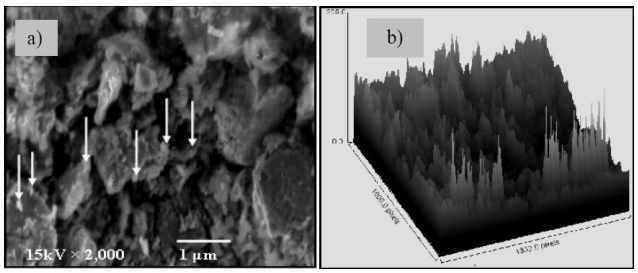

Figure 13 : (a) SEM micrograph and (b) Surface plot of a selected area of a SEM image acquired from Fe/CTC at 800 °C in (He)

COCLUSIONS

In summary, the nanosized carbon materials containing iron and cobalt nano- particles were successfully synthesized by a modified carbon materials approach and deposited by MPCVD technique. XRFM characterization showed that our system of high homogeneous elemental distribution on the surface and overall the sub layer surface. The as-resulting particles exhibit by XRD analysis amorphous structure of these complexes and crystals of iron and cobalt aluminum carbides have been successfully synthesized. The comparison of the DLS results of both complexes Fe and Co carbon materials showed that the particle size of cobalt increased than the particle size of iron sample at 70 ˚C over the time of the experiment. Interestingly, for the UV results depict in the case of Co/CTC, showed that there is a red shift as compared to Fe/CTC -110 which are in a good agreement with the DLS studies. It can be more specifically from the SEM results that, higher calcinations temperatures resulted in crystallite growth and agglomeration for samples treated in air, however for the samples treated in inert atmosphere (He) confirmed the presence of carbon nanoparticles. It can be concluded that at high temperatures the rate of carbon nucleation was too fast compared to that of precipitation resulting to a rapid encapsulation of the catalyst particles with a concomitant formation of carbon nanoparticles.

REFERENCES

[1] Royal Society, Royal Academy for Engineering, Nanoscience and Nanotechnologies: Opportunities and Uncertainties, chapter 2, The Royal Society, London, UK, **(2004)**.

[2] M.Salavati-Niasari, H.Babazadeh-Arani; Cyclohexene oxidation with tert-butylhydroperoxide and hydrogen peroxide catalyzed by new square-planar manganese (II), cobalt (II), nickel (II) and copper (II) bis (2-mercaptoanil)benzil complexes supported on alumina, J.Mol.Catal.A, Chem., **274**, 58–64 **(2007)**.

[3] G.Ennas, A.Falqui, G.Paschina, G.Marongiu; Iron-Cobalt Alloy Nanoparticles Embedded in an Alumina Xerogel Matrix, J.Chem.Mater, **17**, 6486–6491 **(2005)**.

[4] N.S.Babu, N.Lingaiah, J.V.Kumar, P.S.S.Prasad; Studies on alumina supported Pd-Fe bimetallic catalysts prepared bydeposition-precipitation method for hydrodechlorination of chlorobenzene, J.Appl.Catal. A:Gen., **367**, 70–76 **(2009)**.

[5] F.N.Aguero, B.P.Barbero, L.Gambaro, L.E.Cadús; J.Appl.Catal.B: Environ, **91**, 108–112 **(2009)**.

Full Paper

[6] S.Enthaler, K.Junge, M.Beller; Sustainable metal catalysis with iron: from rust to rising star, J.Angew.Chem.Int.Ed.Engl., **47(18)**, 3317–21 **(2008)**.

[7] A.B.M.Giasuddin, S.R.Kanel, H.Choi; Adsorption of humic acid onto nanoscale zerovalent iron and its effect on arsenic removal, J.Environ.Sci.Technol., **41(6)**, 2022–7 **(2007)**.

[8] P.C.Wu, Y.D.Kuo, E.H.Yao, Tsai; Magnetic and optical properties of Fe_3O_4 nanoparticle ferroûuids prepared by coprecipitation technique, J.IEEE.Trans.Magn., **37(4I)**, 2651–3 **(2001)**.

[9] A.N.Shipway, E.Katz, I.Willner; Nanoparticle arrays on surfaces for electronic, optical, and sensor applications, Chemphyschem, **1(1)**, 18–52 **(2000)**.

[10] N.Tran, R.Pareta, E.Taylor, T.J.Webster; Iron oxide nanoparticles: novel drug delivery materials for treating bone diseases, J.Adv.Mater.Res., **89–91**, 411–8 **(2010)**.

[11] B.Chertok, B.A.Moffat, A.E.David, F.Yu, C.Bergemann, B.D.Ross; Iron oxide nanoparticles as a drug delivery vehicle for MRI monitored magnetic targeting of brain tumors, J.Biomaterials, **29(4)**, 487–96 **(2008)**.

[12] D.L.Huber; Synthesis, properties, and applications of iron nanoparticles, J.Small, **1(5)**, 482–501 **(2005)**.

[13] B.H.Davis; Fischer–Tropsch synthesis: relationship between iron catalyst composition and process variables, J.Catal Today, **84(1–2)**, 83–98 **(2003)**.

[14] F.Jaouen, S.Marcotte, J.P.Dodelet, G.Lindbergh; Oxygen reduction catalysts for polymer electrolyte fuel cells from the pyrolysis of iron acetate adsorbed on various carbon supports, J.Phys.Chem.B, **107(6)**, 1376–86 **(2003)**.

[15] G.Bian, A.Oonuki, A.Kobayashi, N.Koizumi, M.Yamada; Syngas adsorption on precipitated iron catalysts reduced by H_2, syngas or CO and on those used for high-pressure FT synthesis by in situ diffuse reflectance FTIR spectroscopy, J.Appl.Catal.A.Gen., **219(1–2)**, 13–24 **(2001)**.

[16] H.Y.Lin, Y.W.Chen, W.J.Wang, Preparation of nanosized iron oxide and its application in low temperature CO oxidation, J.Nanopart.Res., **7(2–3)**, 249–63 **(2005)**.

[17] H.C.Wang, S.H.Chang, P.C.Hung, J.F.Hwang, M.B.Chang; Catalytic oxidation of gaseous PCDD/Fs with ozone over iron oxide catalysts, J.Chemosphere, **71(2)**, 388–97 **(2008)**.

[18] Wei-xian Zhang; Nanoscale iron particles for environmental remediation: An overview, Journal of Nanoparticle Research, **5**, 323–332 **(2003)**.

[19] T.Hu, J.Juuti, H.Jantunen, T.Vilkman; Dielectric properties of BST/polymer Composite, J.Eur.Ceram.Soc, **27**, 3997–4001 **(2007)**.

[20] Kh.D.Ibragimov, E.G.Ismailov, G.S.Martynova, N.R.Bektashi, Z.M.Ibragimova, M.I.Rustamov; Synthesis of a Component of the Jet Engine Fuel and an Accelerator of Oil Tar Oxidation by Catalytic Processing of Heavy Pyrolysis Tar, Russian Journal of Applied Chemistry, **83(7)**, 1159-1163 **(2010)**.

[21] P.Van der Meeren, H.Bogaert, J.Vanderdeelen, L.Baert; Relevance of light-scattering theory in photon-correlation spectroscopic experiments, J.Particle & Particle Systems Characterization, **9**, 138–143 **(1992)**.